Inorg. Chem. **2006**, *45*, 732–743

Stable 8-Hydroxyquinolinate-Based Podates as Efficient Sensitizers of Lanthanide Near-Infrared Luminescence

Steve Comby, Daniel Imbert,* Anne-Sophie Chauvin, and Jean-Claude G. Bünzli

Laboratory of Lanthanide Supramolecular Chemistry, École Polytechnique Fédérale de Lausanne (EPFL), BCH 1402, CH-1015 Lausanne, Switzerland

Received September 7, 2005

New polydentate ligands (e.g., **Tsox** and **TsoxMe)** have been synthesized to take advantage of the chelating effect of bidentate 8-hydroxyquinolinate subunits connected to a *N,N,N′,N′*-tetraaminopropyl-1,2-ethylenediamine framework and with the aim of sensitizing the NIR luminescence of Nd^{III} and Yb^{III} ions. Ten pK_a's have been determined and the interaction between the ligands and Ln^{III} ions in dilute aqueous solution has been probed both by potentiometric and spectrophotometric titrations. These studies have been mostly performed with the Eu^{III} ion, which is in the middle of the lanthanide series, and extended to other ions (La^{III}, Er^{III}, Lu^{IIII}). Stable complexes with Ln^{III} ions are formed (pLn in the range of 14–16), the four chromophoric units being coordinated to the metal center, exploiting the entropic effect generated by the anchor. The monometallic complexes $[Ln(H_2L)]^{3-}$ exist as the major species at physiological pH regardless of the lanthanide used. Lifetime determinations of the Nd($^4F_{3/2}$) and Yb($^2F_{5/2}$) excited levels in both H_2O and D_2O at buffered pH point to the absence of water molecules bound in the inner coordination sphere of the Ln^{III}. Photophysical properties of the free ligands and of their lanthanide complexes have been investigated in buffered aqueous solutions both at room temperature and 77 K. The low-energy triplet state makes energy transfers from the ligand to the metal ions possible; this leads to a sizable sensitization of the Nd^{III}- or Yb^{III}-centered luminescence ($Q^L_{Nd} = 0.02\%$ and $Q^L_{Yb} = 0.18\%$) for **Tsox** chelates. Methylation of the amide functions removes the quenching mechanism induced by the proximate N–H vibrations and increases both the lifetimes and quantum yields of the **TsoxMe** chelates ($Q^L_{Nd} = 0.04\%$ and $Q^L_{Yb} = 0.37\%$). In fact, **TsoxMe** yields one of the most luminescent Yb^{III} compounds known in water, and this ligand appears to be suitable for the development of NIR probes for bioanalyses.

Introduction

Diagnostic imaging technologies developed over the past thirty years, such as magnetic resonance imaging and X-ray or nuclear tomography, revolutionized clinical medicine. Several parameters influence the final result: resolution, depth penetration, availability of biocompatible and targeted probes, and the detection threshold of the latter.[1] During the past decade, in vivo optical detection of tumors by means of near-infrared (NIR) photons has gained momentum[2−4] because it represents a noninvasive technique allowing the exploration of deeper tissues, the investigation range extending from a few millimeters up to 20 cm.[5] Indeed, biological tissues have very low absorption coefficients above 700 nm, and in addition, the absorption of water, a major component of biological tissues, diminishes drastically above 900 nm. The development of targeted NIR fluorophores coupled to peptides prompted applications in clinical situations where other imaging techniques are not an option. Until now, most of these clinical applications have made use of organic dyes as probes for NIR imaging, and differentiation between the target and background fluorescence has been achieved by molecular switches or beacons (protease-triggered NIR probes) which can be activated in vivo by a suitable biochemical reaction.[1]

* To whom correspondence should be addressed. E-mail: Daniel.imbert@epfl.ch.

(1) Weissleder, R. *Nature Biotech.* **2001**, *19*, 316−317.
(2) Weissleder, R.; Tung, C. H.; Mahmood, U.; Bogdanov, A. *Nature Biotech.* **1999**, *17*, 375−378.
(3) Becker, A.; Hessenius, C.; Licha, K.; Ebert, B.; Sukowski, U.; Semmler, W.; Wiedenmann, B.; Grotzinger, C. *Nature Biotech.* **2001**, *19*, 327−331.
(4) Kim, S.; Lim, Y. T.; Soltesz, E. G.; De Grand, A. M.; Lee, J.; Nakayama, A.; Parker, J. A.; Mihaljevic, T.; Laurence, R. G.; Dor, D. M.; Cohn, L. H.; Bawendi, M. G.; Frangioni, J. V. *Nature Biotech.* **2004**, *22*, 93−97.
(5) Weissleder, R.; Ntziachristos, V. *Nature Med.* **2003**, *9*, 123−128.

10.1021/ic0515249 CCC: $33.50 © 2006 American Chemical Society
Published on Web 12/24/2005

An alternate strategy would be to resort to bioprobes incorporating NIR-emitting lanthanide ions,[6] such as Nd^{III} with fluorescence lines in three distinct spectral ranges, 0.87−0.92, 1.06−1.09, and 1.32−1.39 μm ($^4F_{3/2} \rightarrow {}^4I_{9/2}$, $^4I_{11/2}$, $^4I_{13/2}$ transitions), or Yb^{III} which gives off light in the range of 0.98−1.03 μm ($^2F_{5/2} \rightarrow {}^2F_{7/2}$ transition). As for the visible-emitting Ln^{III} ions, which are well-known optical probes,[7−9] the main advantages of these ions lie in their easily recognizable atom-like spectra and large Stokes shifts. In addition, time-resolved luminescence permits a high signal-to-noise ratio since the lifetimes of the emissive states are usually long, in the microsecond to millisecond range for phosphorescent ions such as Sm^{III}, Eu^{III}, and Tb^{III}. Synthetic strategies are now at hand to insert Ln^{III} ions in a variety of molecular and supramolecular assemblies[10] which control and even enhance their photophysical properties through the so-called antenna effect (or sensitization process) since f−f transitions have oscillator strengths which are too weak to yield an efficient excitation path.[7] Finally, bi- and polymetallic edifices may also be conveniently designed, which opens the way to polyfunctional probes.[11] The NIR luminescent ions have been the focus of many studies for various reasons, one being their use in telecommunication and laser design.[12,13] With respect to bioprobes, Yb^{III} has attracted a wealth of attention; for instance, the Cotton effect displayed by the $^2F_{5/2} \leftarrow {}^2F_{7/2}$ transition has been used to study antibiotics,[14] the circularly polarized emission $^2F_{5/2} \rightarrow {}^2F_{7/2}$ has been proposed for chiral assays of biological structures,[15] and a NIR-emissive protein conjugate has been applied in medical diagnostics.[16] Other ions, such as Nd^{III} can also be useful, as demonstrated by the design of hairpin-shaped heterometallic complexes for DNA intercalation.[17] Recently, sensitization of the NIR luminescence of Nd^{III}, Ho^{III}, Er^{III}, Tm^{III}, and Yb^{III} has been achieved by tropolonate ligands.[18] With respect to the visible-emitting Ln^{III} ions, those displaying NIR luminescence have two intrinsic drawbacks: (i) comparatively shorter lifetimes (ns−μs), which somewhat limit the efficiency of time-resolved experiments, and (ii) they are more amenable to nonradiative deactivation because they have a smaller energy gap between their emissive and ground states. The first disadvantage can be overcome by the use of d-transition metal ions for the population of the excited states of the 4f ions; for instance, we have recently shown that introducing the NIR-emitting Nd^{III} and Yb^{III} ions into 3d−4f bimetallic edifices allows the control of the population of the Ln^{III} excited state by the long-lived emitting Cr^{III} ion.[19,20] Here, we develop a strategy to address the second problem, with achieving good sensitization of the NIR luminescence in aqueous solutions as the goal, an obvious requirement for potential in vivo applications.

A good way to obtain efficient energy transfer from the ligand onto the NIR-emitting metal ion while simultaneously achieving thermodynamic stability and kinetic inertness of the resulting molecular edifice is to resort to multidentate podands fitted with one or several sensitizer arms.[21,22] It is essential that the targeted chelating agents offer a good protection against solvent interactions and are devoid of coordinating groups possessing high-energy vibrations, the latter being efficient quenchers of the Ln^{III} luminescence. With ions such as Nd^{III} and Yb^{III}, the reported quantum yields in water are usually smaller than 0.1%.[18,23] To our knowledge, the only exception is a bimetallic Yb^{III} complex with 1,10-phenanthroline substituted in the 2 and 9 positions by benzo-azacyclic moieties which has $Q_{Ln}^{L} = 0.53\%$ in water.[24] Our ligand design (**Tox**) relies on a short 1,2-diaminoethane backbone fitted with four 8-hydroxyquinoline moieties since the corresponding anion is known to be an efficient sensitizer of Ln^{III} NIR luminescence.[25,26] The spacer bears an amide coupling function, and its length has been chosen to achieve a tight coordination environment around the Ln^{III} ion. To improve solubility, sulfonate groups have been grafted onto the 8-hydroxyquinoline building block yielding a second ligand, **Tsox**. We have shown, in a preliminary communication, that this design leads to 1:1 complexes with large thermodynamic stability in aqueous solution and no water molecule bound in the inner coordination sphere.[27] Here, we report the full thermodynamic and photophysical properties of these ligands and of their complexes with Ln^{III} (Ln = La, Nd, Eu, Gd, Tb, Er, Yb and Lu) and propose a modification of the initial ligand framework, by methylation of the nitrogen atom of the amide

(6) Faulkner, S.; Pope, S. J. A.; Burton-Pye, B. P. *Appl. Spectrosc. Rev.* **2005**, *40*, 1−31.
(7) Bünzli, J.-C. G.; Piguet, C. *Chem. Soc. Rev.* **2005**, *34*, 1048.
(8) Bünzli, J.-C. G. In *Spectroscopic Properties of Rare Earths in Optical Materials*; Liu, G. K., Jacquier, B., Eds.; Springer-Verlag: Berlin, 2005, 11; pp 462−499.
(9) Bünzli, J.-C. G. In *Metal Complexes in Tumor Diagnosis and as Anticancer Agents*; Sigel, A., Sigel, H., Eds.; Marcel Dekker Inc.: New York, 2004; pp 39−75.
(10) Piguet, C.; Bünzli, J.-C. G. *Chem. Soc. Rev.* **1999**, *28*, 347−358.
(11) Bünzli, J.-C. G.; Piguet, C. *Chem. Rev.* **2002**, *102*, 1897−1928.
(12) Van Deun, R.; Nockemann, P.; Görller-Walrand, C.; Binnemans, K. *Chem. Phys. Lett.* **2004**, *397*, 447−450.
(13) Stouwdam, J. W.; Van Veggel, F. C. J. M. *Nano Lett.* **2002**, *2*, 733−737.
(14) Salvadori, P.; Rossini, C.; Bertucci, C. *J. Am. Chem. Soc.* **1984**, *106*, 2439.
(15) Maupin, C. L.; Dickins, R. S.; Govenlock, L. G.; Mathieu, C. E.; Parker, D.; Williams, J. A. G.; Riehl, J. P. *J. Phys. Chem. A* **2000**, *104*, 6709−6717.
(16) Werts, M. H. V.; Woudenberg, R. H.; Emmerink, P. G.; van Gassel, R.; Hofstraat, J. W.; Verhoeven, J. W. *Angew. Chem., Int. Ed.* **2000**, *39*, 4542−4544.
(17) Glover, P. B.; Ashton, P. R.; Childs, L. J.; Rodger, A.; Kercher, M.; Williams, R. M.; De Cola, L.; Pikramenou, Z. *J. Am. Chem. Soc.* **2003**, *125*, 9918−9919.
(18) Zhang, J.; Badger, P. D.; Greib, S. J.; Petoud, S. *Angew. Chem., Int. Ed.* **2005**, *44*, 2508−2512.
(19) Torelli, S.; Imbert, D.; Cantuel, M.; Bernardinelli, G.; Delahaye, S.; Hauser, A.; Bünzli, J.-C. G.; Piguet, C. *Chem. Eur. J.* **2005**, *11*, 3228−3242.
(20) Imbert, D.; Cantuel, M.; Bünzli, J.-C. G.; Bernardinelli, G.; Piguet, C. *J. Am. Chem. Soc.* **2003**, *125*, 15698−15699.
(21) Beeby, A.; Burton-Pye, B. P.; Faulkner, S.; Motson, G. R.; Jeffery, J. C.; McCleverty, J. A.; Ward, M. D. *J. Chem. Soc., Dalton Trans.* **2002**, 1923−1928.
(22) Beeby, A.; Bushby, L. M.; Maffeo, D.; Williams, J. A. G. *J. Chem. Soc., Dalton Trans.* **2002**, 48−54.
(23) Werts, M. H. V.; Verhoeven, J. W.; Hofstraat, J. W. *J. Chem. Soc., Perkin Trans. 2* **2000**, 433−439.
(24) Korovin, Y. V.; Rusakova, N. V.; Popkov, Y. A.; Dotsenko, V. P. *J. Appl. Spectrosc.* **2002**, *69*, 841−844.
(25) Rizzo, F.; Papagni, A.; Meinardi, F.; Tubino, R.; Ottonelli, M.; Musso, G. F.; Dellepiane, G. *Synth. Met.* **2004**, *147*, 143−147.
(26) Kido, J.; Okamoto, Y. *Chem. Rev.* **2002**, *102*, 2357−2368.
(27) Imbert, D.; Comby, S.; Chauvin, A.-S.; Bünzli, J.-C. G. *Chem. Commun.* **2005**, 1432−1434.

function (**TsoxMe**) to obtain better photophysical properties by minimizing nonradiative deactivation through proximate N−H groups.

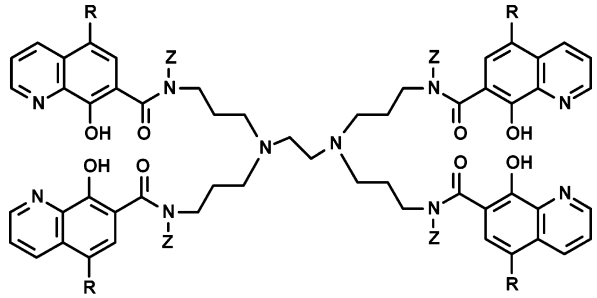

R = H, Z = H Tox
R = SO_3^- Z = H Tsox = $(H_4L)^{4-}$
Z = Me TsoxMe = $(H_4L^{Me})^{4-}$

Materials and Methods

Starting Materials and General Procedures. Tetrahydrofuran (99+% from Acros) and methanol (99.9% from Merck) were purified by the usual techniques.[28] Chloroform-*d* (99.8 at. % D) and dimethyl-d_6 sulfoxide (99.8 at. % D) from *Armar Chemicals* and deuterium oxide (99.9 at. % D) from Aldrich were used for ^{1}H and ^{13}C NMR spectra which were performed on a Bruker Avance DRX 400 spectrometer at 25 °C, using deuterated solvents as internal standards. Mid-infrared spectra were recorded using a Perkin-Elmer Spectrum One spectrometer equipped with a universal attenuated total reflection sampler. ESI-MS spectra were obtained on a Finningan SSQ 710C spectrometer using 10^{-5}−10^{-4} M solutions in acetonitrile/H_2O/acetic acid (50/50/1), a capillary temperature of 200 °C, and an acceleration potential of 4.5 keV. The instrument was calibrated using horse myoglobin, and all analyses were conducted in positive mode; the ion-spray voltage was 4.6 keV. ESI-Tof spectra were measured with a Q-Tof Ultima mass spectrometer (Micromass, Manchester, UK) equipped with a Z-spray type ESI source. Phosphoric acid was used for the negative ion mass calibration range of 100−2000 *m*/*z*. Data were acquired and processed using Masslynx version 4.0. Electrospray conditions were as follows: capillary voltage, 3 kV; source temperature, 80 °C; cone voltage, 35 V; source block temperature, 150 °C. The ESI nebulization and drying gas was nitrogen. All experiments were performed in the negative ion mode. The samples were introduced via a syringe pump operating at 20 μL/min. Elemental analyses were performed by Dr. H. Eder from the Microanalytical Laboratory of the University of Geneva.

Physicochemical Measurements. Analytical grade solvents and chemicals (Fluka AG) were used without further purification. The HBS buffer was prepared by mixing a 10 mM solution of HEPES and a 150 mM solution of NaCl (in doubly distilled water). Stock solutions of lanthanides were prepared just before use in freshly boiled, doubly distilled water from the corresponding perchlorate salts, $Ln(ClO_4)_3 \cdot nH_2O$ (Ln = La, Nd, Eu, Gd, Tb, Er, Yb and Lu; n = 3−6). ***Caution****: Perchlorate salts combined with organic ligands are potentially explosive and should be handled in small quantities and with adequate precautions.*[29,30] These salts were prepared from their oxides (Rhône-Poulenc, 99.99%) in the usual manner.[31] Concentrations of the solutions were determined by complexometric titrations using a standardized Na_2H_2EDTA solution in urotropine buffered medium and with xylenol orange as the indicator.[32] UV−vis absorption spectra were measured on a Perkin-Elmer Lambda 900 spectrometer using quartz Suprasil cells of 0.2 and 1 cm path lengths.

Spectrophotometric Titrations. Spectrophotometric titrations were performed with a J&M diode array spectrometer (Tidas series) connected to an external computer. All titrations were performed in a thermostated (25.0 ± 0.1 °C) glass-jacketed vessel at μ = 0.1 M (KCl). In a typical experiment, 50 mL of a ligand solution (5×10^{-6} M) was titrated with freshly prepared sodium hydroxide solutions at different concentrations (4, 1, 0.1, and 0.01 M). After each addition of base, the pH of the solution was measured by a KCl-saturated electrode, and the UV−vis absorption spectrum was recorded using a 1 cm Hellma optrode immersed in the thermostated titration vessel and connected to the Tidas spectrometer. The same conditions were used for the titration of stoichiometric 1:1 quantities of $Eu(ClO_4)_3 \cdot nH_2O$ and the **Tsox** ligand. Solutions were systematically acidified with HCl before metal addition to avoid hydroxide precipitation. Using the same equipment, we determined conditional stability constants by titration of **Tsox** with Ln^{III} at a fixed pH (0.1 M HBS buffer, pH 7.4) and of **Tox** in methanol (μ = 0.1 M with TEAP) after deprotonation by 4 equiv of KOH (1 M in EtOH). Factor analysis[33] and mathematical treatment of the spectrophotometric data were performed with the SPECFIT program.[34,35]

Potentiometric Titrations. Tsox or **TsoxMe** $(H_{10}L)^{2+}$ were titrated using a 5 mL sample ($[H_{10}L^{2+}]_{tot} = 9.41 \times 10^{-4}$ M in H_2O) in a thermostated (25.0 ± 0.1 °C) glass-jacketed vessel under an Ar atmosphere. The ionic strength was fixed with KCl (μ = 0.1 M). The solution was acidified to a pH of ∼1.7 with fuming HCl 30 min before titration. Titrations were carried out with an automatic Metrohm Titrino 736 GP potentiometer linked to an IBM PS/2 computer (resolution 0.1 mV, accuracy 0.2 mV) using constant volume addition (0.025 mL). An automatic buret (Metrohm 6.3013.210, 10 mL, accuracy 0.03 mL) was used along with a Metrohm 6.0238.000 glass electrode. The standard base solution (0.1 M NaOH) was added inside the solution through a capillary tip attached to the automatic buret. The data (200 points, drift < 1 mV/min) were mathematically treated by the program HYPERQUAD2000[36,37] using a Marquardt algorithm, while the distribution of species was calculated with the program HYSS2. Calibration of the pH meter and the electrode system was performed prior to each measurement using a standardized HCl solution at 25.0 °C: 10 mL of the latter were titrated with a standardized 0.1 M NaOH solution, and the electrode potential readings were converted to pH. The ion product of water (pK_w = 13.91) and electrode potential were refined using the program Scientist by Micromath (version 2.0).

Luminescence Measurements. Low-resolution luminescence measurements (spectra and lifetimes) were recorded on a Fluorolog

(28) Perrin, D. D.; Armarego, W. L. F. *Purification of Laboratory Chemicals*; Pergamon Press: Oxford, 1988.
(29) Wolsey, W. C. *J. Chem. Educ.* **1973**, *50*, A335−A337.
(30) Raymond, K. N. *Chem. Eng. News* **1983**, *61*, 4.
(31) Desreux, J. F. In *Lanthanide Probes in Life, Chemical and Earth Sciences. Theory and Practice*; Bünzli, J.-C. G., Choppin, G. R., Eds.; Elsevier Science: Amsterdam, 1989; Chapter 2, pp 43−64.
(32) Schwarzenbach, G. *Complexometric Titrations*; Chapman & Hall: London, 1957; pp 8−ff.
(33) Malinowski, E. R.; Howery, D. G. *Factor Analysis in Chemistry*; John Wiley: New York, 1991.
(34) Gampp, H.; Maeder, M.; Meyer, C. J.; Zuberbühler, A. D. *Talanta* **1985**, *32*, 95−101.
(35) Gampp, H.; Maeder, M.; Meyer, C. J.; Zuberbühler, A. D. *Talanta* **1986**, *33*, 943−951.
(36) Sabatini, A.; Vacca, A.; Gans, P. *Coord. Chem. Rev.* **1992**, *120*, 389−405.
(37) Alderighi, L.; Gans, P.; Ienco, A.; Peters, D. C.; Sabatini, A.; Vacca, A. *Coord. Chem. Rev.* **1999**, 311−318.

Scheme 1[a]

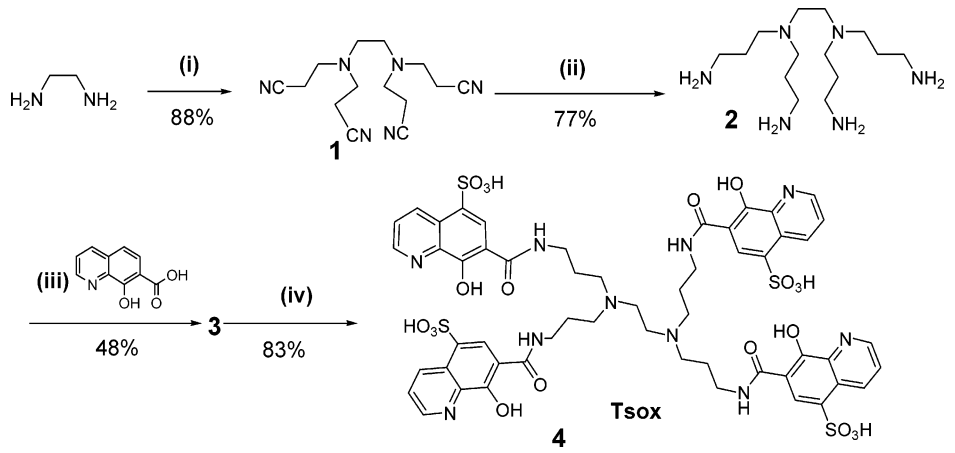

[a] (i) CH_2CHCN, H_2O; (ii) Raney nickel, hydrazine, ethanol; (iii) 7-carboxy-8-hydroxyquinoline, CDI, thf; (iv) H_2SO_4, SO_3 (20%).

FL 3-22 spectrometer from Spex-Jobin-Yvon-Horiba with double-grating emission and excitation monochromators and a R928P photomultiplier. For measurement in the NIR spectral range, the spectrometer was fitted with a second measuring channel equipped with a FL-1004 single-grating monochromator, and the light intensity was measured by two Jobin-Yvon solid-state InGaAs detectors, (i) DSS-IGA020L, cooled to 77 K (800−1600 nm range) and (ii) DSS-IGA020A (800−1700 nm) working at room temperature, inserted into a LN2 housing including an elliptical mirror (90° beam path) and coupled to a Jobin Yvon SpectrAcq2 data acquisition system. Samples were put in 1 cm path length quartz Suprasil cells, and the temperature was kept constant at 25.0 ± 0.1 °C using a FL-1027 thermostated cell holder connected to a water bath. All spectra were corrected for the instrumental functions. Phosphorescence lifetimes (τ) were measured in frozen glycerol/water solutions (10/90%) in time-resolved mode. They are averages of three independent measurements, which were made by monitoring the decay at the maxima of the emission spectra, enforcing a 0.05−0.5 ms delay. The monoexponential decays were analyzed with Origin 7.0. Quantum yields (Q^L_{Ln}) of the complexes at pH 7.4 (HBS buffer) and room temperature were determined relative to those of $Cs_3[Eu(dpa)_3]$, $Q^L_{EU} = 13.5\%$,[38] for complexes emitting in the visible region (dpa = dipicolinate) and to those of $[Yb(tta)_3(H_2O)_2]$ (tta = thenoyltrifluoroacetylacetonate) in toluene, $Q^L_{Yb} = 0.35\%$,[39] for the NIR-emitting complexes. The estimated error is ±10%. Quartz Suprasil cells with a 0.2 cm path length were used for these measurements.

The general layout of the instrumental setup for the high-resolution emission spectra in the NIR region was as follows. All components are connected to a controller PCI card which, in turn, transfers information to and from the computer and allows data treatment through an application developed in the laboratory with Labview 7.0 software from National Instrument. Three types of excitation light sources linked to optical fibers from Optonet were used: (i) a Zeiss XBO 450 W xenon high-pressure lamp coupled with a 1/4 M 77200 monochromator from Oriel controlled by a specially designed stepper motor and shutter unit for broad-band excited emission and excitation spectra, (ii) a tunable Coherent CR-599 dye laser (band path 0.03 nm, 50−300 mW) pumped by a continuous Coherent Innova-90 argon laser (8 W) for which the lines at 465.8, 488, and 514 nm were used, and (iii) an OPOTEK Vibrant 355 I tunable laser system including a Quantel Brillant Nd:YAG laser (330 mJ at 1064 nm) equipped with frequency doubler (160 mJ at 532 nm), tripler (110 mJ at 355 nm), and quadrupler (54 mJ at 266 nm) and a MagicPrism^T OPO crystal (line width 2−15 cm^{-1}, 25−54 mJ from 410 to 690 nm and 2−12 mJ from 720 to 2400 nm) pumped at 355 nm.

The emitted light was analyzed at 90° with a Spex 1870 single monochromator with 950 g/mm holographic gratings blazed at 900 nm. Light intensity was measured by a cooled NIR PMT Module H9170-75 photomultiplier from Hamamatsu equipped with an A9176MOD adaptor and coupled to a Stanford Research SR-400 double-photon counter for emission spectra. For lifetime determinations, the output signal of the photomultiplier was fed into a Lecroy LT262 oscilloscope (1 GHz) to avoid saturation of the signal and then into a Standford Research SR-430 multichannel scaler. Data were transferred into a PC and corrected for the instrumental function. Low-temperature measurements were performed with the help of a CTI−Cryogenics Cryodyne M-22 closed-cycle refrigerator controlled by a Lakeshore 321 temperature controller.

Results and Discussion

Ligands **Tox** and **Tsox** were obtained according to the synthetic pathway depicted in Scheme 1. Compound **1** was prepared as previously described[40] and was reduced[41] using Raney nickel to give the tetraamine **2**. In the next step, the latter product was condensed with activated 7-carboxy-8-hydroxyquinoline to give the tetrapodal ligand **Tox**. Finally, regiospecific sulfonation of the 8-hydroxyquinoline subunits was achieved using oleum, as already reported for 2-carboxy-8-hydroxyquinoline,[42] yielding **Tsox** with an overall yield of 32% over four steps. Methylation of the amide functions of tetraamide **2**[43] led to **TsoxMe** (Scheme 2). Synthetic procedures are detailed in the Supporting Information.

Ligand Deprotonation Constants. The fully protonated **Tsox** ligand possesses fourteen deprotonation sites, four

(38) Chauvin, A.-S.; Gumy, F.; Imbert, D.; Bünzli, J.-C. G. *Spectrosc. Lett.* **2004**, *37*, 517−532.
(39) Tsvirko, M. P.; Meshkova, S. B.; Venchikov, V. Y.; Bol'shoi, D. V. *Opt. Spectrosc. (Engl. Transl.)* **1999**, *87*, 866−870.
(40) van Duijvenbode, R. C.; Rajanayagam, A.; Koper, G. J. M.; Borkovec, M.; Paulus, W.; Steuerle, U.; Haussling, L. *Phys. Chem. Chem. Phys.* **1999**, *1*, 5649−5652.
(41) Imbert, D.; Thomas, F.; Baret, P.; Serratrice, G.; Gaude, D.; Pierre, J. L.; Laulhere, J. P. *New J. Chem.* **2000**, *24*, 281−288.
(42) Shrader, W. D.; Celebuski, J.; Kline, S. J.; Johnson, D. *Tetrahedron Lett.* **1988**, *29*, 1351−1354.
(43) Schmidt, H.; Lensink, C.; Xi, S. K.; Verkade, J. G. *Z. Anal. Chem.* **1989**, *578*, 75−80.

Scheme 2[a]

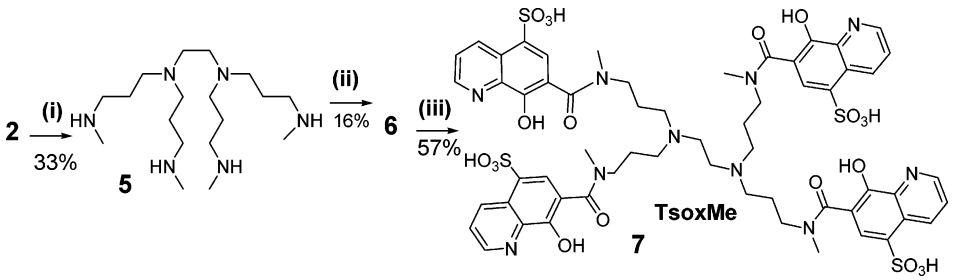

[a] (i) (a) $EtCO_2Cl$, H_2O, toluene, (b) $LiAlH_4$, THF; (ii) 7-carboxy-8-hydroxyquinoline, CDI, thf; (iii) H_2SO_4, SO_3 (20%).

pyridinium nitrogens, two tertiary nitrogen atoms, four hydroxyl oxygen atoms, and four sulfonate groups. The deprotonation constants of **Tsox** were determined separately by potentiometry and spectrophotometry. The sulfonate groups being totally deprotonated under the experimental conditions used, the starting species is written $(H_{10}L)^{2+}$. The extracted pK_a values obtained from titrations in the 1.5−12.5 pH range are defined by the following equations

$$(H_{11-i}L)^{(3-i)+} \rightleftarrows (H_{10-i}L)^{(2-i)+} + iH^+ \quad (1)$$

$$K_{ai} = [H_{10-i}L^{(2-i)+}][H^+]^i/[H_{11-i}L^{(3-i)+}] \quad (i = 1-10) \quad (2)$$

The potentiometric titration of the protonated form $(H_{10}L)^{2+}$ of the ligand in 0.1 M KCl with NaOH at 25 °C (Figure S1, Supporting Information) allowed the determination of only five deprotonation constants because of the precipitation below pH 5.5 which restricted the exploitable data to the pH range of 5.5−12.26. On the other hand, a spectrophotometric titration carried out in the pH range of 1.7−12.5 at lower concentration (Figure 1) allowed us to determine the remaining pK_a's, except for pK_{a2} and pK_{a3} for which only the sum could be calculated; a similar situation prevails for pK_{a7} and pK_{a8}, but the individual values could be calculated from the potentiometric data (Table 1). The absorbance spectra recorded in the pH range of 1.7−7.7 show the presence of three isosbestic points at 242, 276, and 308 nm, while two additional isosbestic points are observed at 249 and 308 nm in the pH range of 7.7−12.5. The calculated spectra are in good agreement with the experimental data, and extractions at different wavelengths are given in Figures S2−S5 (Supporting Information). The corresponding distribution curves obtained from the pK_a values are presented in Figure 2a. In reference to O-Trensox,[44] a tripodal ligand based on sulfonated 8-hydroxyquinoline, the four lowest pK_a values between 1.8 and 4.5 are assigned to the pyridinium nitrogen atoms (1.83, 2.55, and 3.01 for O-Trensox); we note that 5-sulfo-8-hydroxyquinoline has a pK_a value of 3.92.[43] The four pK_a values found between 6.4 and 10.26, with an average of 8.65, are attributed to the hydroxyl moieties. The corresponding values for O-Trensox are in the range of 7.44−8.62, with an average of 8.07, while that of 5-sulfo-8-hydroxyquinoline is 8.42.[44] This difference stems from the presence of an additional arm in **Tsox** than in O-Trensox. Moreover, these four deprotonation constants differ from the statistical factor (log 4 = 0.6) calculated for noninteracting arms, which points to cooperativity taking place between the four arms of the tetrapodal ligand, probably via intra- or intermolecular hydrogen bonds, in contrast to the situation for O-Trensox. The last two deprotonation constants (11.4 and 12.2) come from the tertiary amine groups.

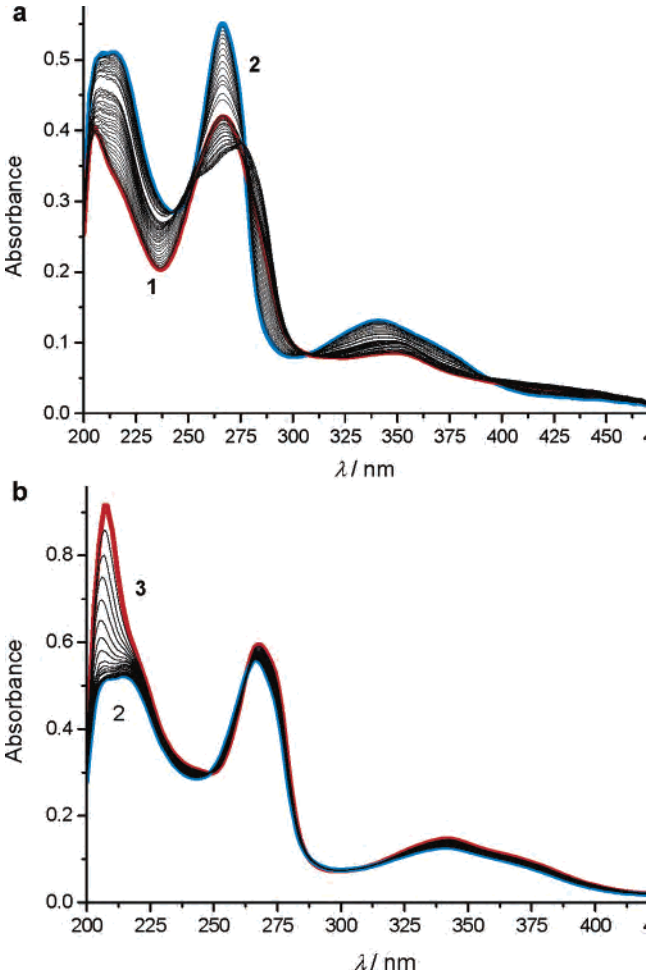

Figure 1. UV−vis absorption spectra of $(H_{10}L)^{2+}$ as a function of pH in water: [**Tsox**] = 5 × 10^{-6} M; T = 25.0 ± 0.1 °C; μ = 0.1 M (KCl). pH values: (1) 1.7, (2) 7.7, (3) 12.5.

Similar experiments were conducted with **TsoxMe** in the pH range of 3.28−12.17 (solubility problems prevented a study at lower pH), and six protonation constants defined by eqs 1 and 2 could be extracted (Table 1). As expected, methylation of the nitrogen atoms of the amide functions does not substantially influence the acidity of the 5-sulfo-8-hydroxyquinoline subunits.

(44) Serratrice, G.; Boukhalfa, H.; Beguin, C.; Baret, P.; Caris, C.; Pierre, J. L. *Inorg. Chem.* **1997**, *36*, 3898−3910.

Table 1. Deprotonation Constants of $(H_{10}L)^{2+}$ ($\pm\sigma$, see eqs 1 and 2 for the definition of K_{ai})

	Tsox			TsoxMe	
	L[a]	L[b]	log β_{10n}[a,b,d]	L[c]	log β_{10n}[c,d]
pK_{a1}		1.8(1)	70.4(1)		
$pK_{a2} + pK_{a3}$		6.0(1)	68.6(1)		
pK_{a4}		4.5(1)	62.6(1)	3.94(14)	62.56(14)
pK_{a5}		6.4(1)	58.1(1)	6.65(11)	58.62(11)
pK_{a6}	8.44(4)	8.7(2)	51.65(4)	8.20(9)	51.97(9)
pK_{a7}	9.46(3)		43.21(3)	9.19(7)	43.77(7)
pK_{a8}	10.26(3)		33.75(3)	11.34(1)	34.58(1)
$pK_{a7} + pK_{a8}$		19.1(1)			
pK_{a9}	11.44(2)	11.4(1)	23.49(2)		
$pK_{a9} + pK_{a10}$				23.24(3)	23.24(3)
pK_{a10}	12.05(2)	12.23(1)	12.05(2)		

[a] Potentiometric data: $[L]_0 = 9.41 \times 10^{-4}$ M, $\mu = 0.1$ M (KCl), $T = 25$ °C. [b] Spectrophotometric data: $[L]_0 = 5.0 \times 10^{-6}$ M, $\mu = 0.1$ M (KCl), $T = 25.0$ °C. [c] Potentiometric data: $[L]_0 = 9.95 \times 10^{-4}$ M, $\mu = 0.1$ M (KCl), $T = 25$ °C. [d] $\beta_{10n} = [(H_{10-i}L)^{(2-n)+}][H+]^i/[(H_{11-n}L)^{(3-n)+}]$.

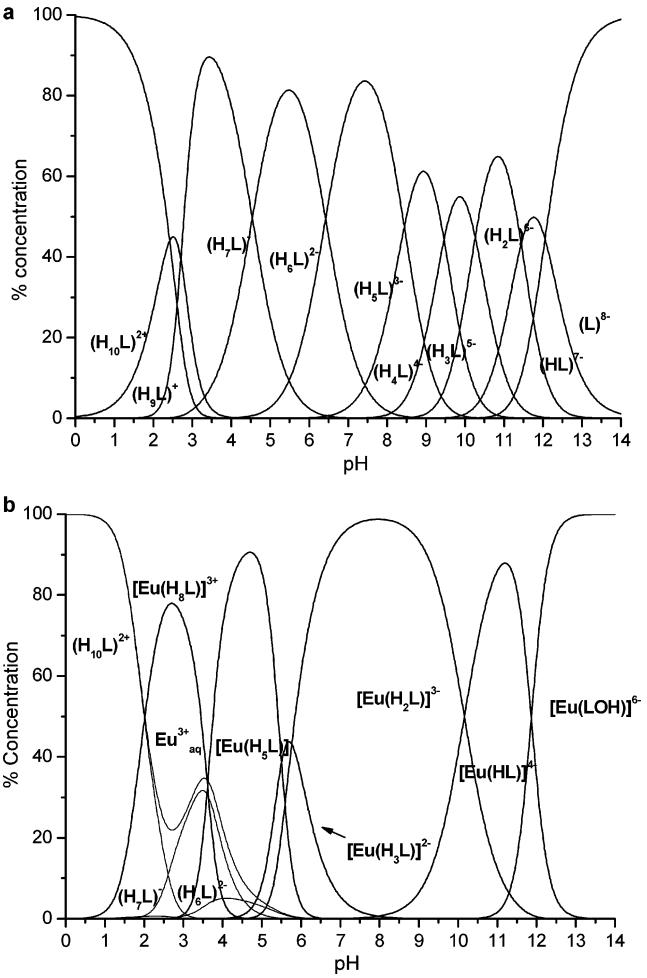

Figure 2. Distribution curves of **Tsox** and Eu-containing species, computed from the (a) pK_a values and (b) stability constants given in text. Calculated for $[L]_{tot} = [Eu^{III}]_{tot} = 10^{-5}$ M, $T = 25$ °C.

Interaction with Trivalent Lanthanide Ions. The nature and stability of the species forming between the Eu^{III} ion and **Tsox** has been first probed at variable pH and in equimolar solutions of ligand and metal ion by potentiometric (pH range 1.72−12.22) and spectrophotometric titrations (pH range 1.71−12.34). This ion was chosen as a typical example because it lies in the middle part of the Ln^{III} series, and in view of the podand nature of the ligands investigated which behave as predisposed receptors, not much difference in the stability of the resulting podates is expected along the lanthanide series.[45,46] The potentiometric titration curve of a 1:1 solution of the Eu^{III} ion and ligand **Tsox** (Figure S6, Supporting Information) shows a pH variation, indicating the release of protons upon Ln^{III} coordination. Furthermore, the formation of hydroxo-complexes is also detected.

Table 2. Cumulative Constants, log β_{11n}, and UV−vis Spectral Characteristic of the Complexes of Eu^{III} (see eqs 3 and 4 for the definition of log β_{11n})

	Tsox				TsoxMe
species	log β_{11n}[a]	log β_{11n}[b]	λ_{max} (nm)[c]	ϵ_{max} (M^{-1} cm^{-1})[d]	log β_{11n}[e]
$[Eu(H_8L)]^{3+}$	–	71.72(1)			
$[Eu(H_5L)]$	61.1(2)	60.98(1)	264	99 420	
			342	19 960	
$[Eu(H_3L)]^{2-}$	–	49.88(3)			50.30(7)
$[Eu(H_2L)]^{3-}$	44.0(2)	44.12(2)	266	92 200	43.22(2)
			342	19 900	
$[Eu(HL)]^{4-}$	33.6(2)	33.98(3)	268	131 500	33.46(1)
			342	26 560	
$[EuL(OH)]^{6-}$	10.0(2)	10.23(5)	268	138 600	9.65(1)
			342	30 370	

[a] Potentiometric data: $[L]_0 = 9.41 \times 10^{-4}$ M, $\mu = 0.1$ M (KCl), $T = 25.0$ °C. [b] Spectrophotometric data: $[L]_0 = 5 \times 10^{-6}$ M, $\mu = 0.1$ M (KCl), $T = 25.0$ °C. [c] ±2 nm. [d] ±10%. [e] Potentiometric data: $[L]_0 = 9.85 \times 10^{-4}$ M, $\mu = 0.1$ M (KCl), $T = 25.0$ °C.

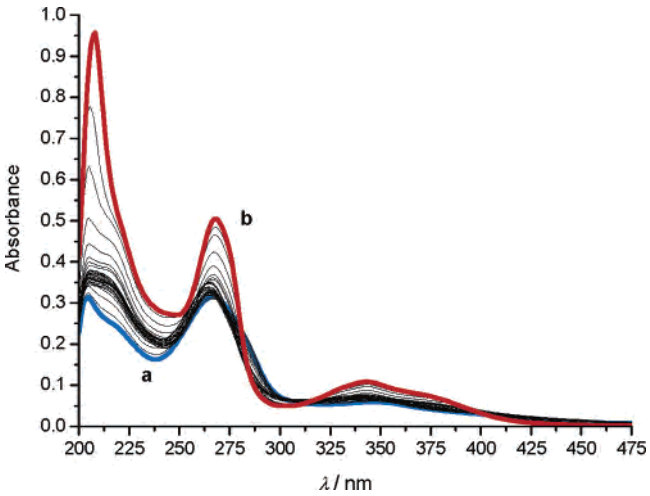

Figure 3. UV−vis absorption spectra of $(H_{10}L)^{2+}$ in the presence of 1 equiv of Eu^{III}: [**Tsox**] = 5×10^{-6} M; $T = 25.0 \pm 0.1$ °C; $\mu = 0.1$ M (KCl). pH values: (a) 1.7, (b) 12.3.

Several models were tested to refine the potentiometric data and the best one involves four complexed species (Table 2). A spectrophotometric titration was then carried out (Figure 3) to correlate the deprotonation constants of the Eu^{III} complex and the cumulative stability constants, β_{11n}, defined by eqs 3 and 4, and the data obtained in two different pH ranges were fitted separately.

$$Ln_{aq}^{3+} + L^{8-} + nH^+ \rightleftarrows [Ln(H_nL)]^{(n-5)+} \quad (3)$$

$$\beta_{11n} = [Ln(H_nL)^{(n-5)+}]/[Ln^{3+}][L^{8-}][H^+]^n \quad (4)$$

Between pH 1.7 and 6, the best fit of the absorbance data corresponds to the presence of only one metal complex,

mainly because several protonated forms of the ligand coexist in this pH range. However, combining these data with the data obtained from the potentiometric titration allowed us to fit the three proton-dependent equilibria described by eqs 5−7

$$Eu_{aq}^{3+} + (H_{10}L)^{2+} \rightleftarrows [Eu(H_8L)]^{3+} + 2H^+ \quad (5)$$

$$[Eu(H_8L)]^{3+} \rightleftarrows [Eu(H_5L)] + 3H^+ \quad (6)$$

$$[Eu(H_5L)] \rightleftarrows [Eu(H_3L)]^{2-} + 2H^+ \quad (7)$$

Above pH 6, both potentiometric and spectrophotometric data point to the presence of three other species. Their stability constants defined by eqs 8−10 were refined by considering two successive deprotonations and the formation of one hydroxo complex at pH higher than 11; they are listed in Table 2. Recalculated spectra and extractions at various wavelengths are shown in Figures S7 and S8 (Supporting Information).

$$[Eu(H_3L)]^{2-} \rightleftarrows [Eu(H_2L)]^{3-} + H^+ \quad (8)$$

$$[Eu(H_2L)]^{3-} \rightleftarrows [Eu(HL)]^{4-} + H^+ \quad (9)$$

$$[Eu(HL)]^{4-} \rightleftarrows [EuL(OH)]^{6-} + 2H^+ \quad (10)$$

Therefore, six different complexes could be found. The corresponding distribution diagram is shown in Figure 2b. Despite the complexity of the system, only one major species (>97%) is present at physiological pH, $[Eu(H_2L)]^{3-}$. The deprotonation constants previously obtained for the ligand and the successive stability constants suggest that the two undissociated protons belong to the tertiary nitrogen atoms, which do not interfere with the coordination sphere. ESI-Tof mass spectra recorded in negative mode on a solution at pH 7.4, prepared by mixing 1 equiv of **Tsox** with 1 equiv of Nd^{III}, Er^{III}, Yb^{III}, and Eu^{III} indeed display a signal corresponding to these species (Figure 4). The other complex present at physiological pH is $[Eu(H_3L)]^{2-}$; upon an increase in the pH, deprotonation of the major species leads to the formation of $[Eu(HL)]^{4-}$ which becomes the major species at pH 11. Further scrutiny of the distribution curves shows a steep decrease of the free Eu^{III} concentration from pH 1 to 2.8 followed by a slight increase up to a pH of ∼3.6 before it completely disappears at pH > 6. This suggests a change in the coordination around the metal ion, as observed for the ferric complex with O-Trensox.[44] Kinetic studies on the latter have demonstrated a preorganization of the ligand at low pH with salicylate-type coordination (carbonyl and phenol) followed, above pH 3, by oxinate-type coordination (phenol and pyridine).

In a second step, the strength of the interaction between several Ln^{III} ions (Ln = La, Eu, Er, Lu) and **Tsox** was monitored by UV−vis spectrophotometry in dilute aqueous solutions at pH 7.4, where the $[Eu(H_2L)]^{3-}$ complex is the

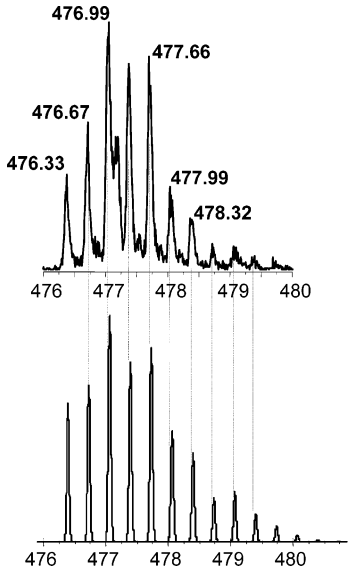

Figure 4. (top) ESI-Tof spectrum of the 1:1 Nd^{III} chelate in water at pH 7.4 and room temperature. (bottom) Recalculated spectrum of the $[NdH_2L]^{3-}$ species using the IsoPro 3.0 MS/MS software.

major species. The conditional stability constants show little variation along the series, which is a clear indication that because of the long arms of the podand, steric effects play a negligible role. In parallel, titrations of the nonsulfonated ligand **Tox** in methanol, after deprotonation of the phenol groups by 4 equiv of KOH gave conditional stability constants smaller by about 2 orders of magnitude pointing to a much more efficient complexation of the Ln^{III} metal ions by the sulfonated ligand **Tsox**. This feature results from the electroattracting effect of the sulfonate groups, leading to a weakening of the O−H phenol bond which facilitates coordination of the metal ions.

The complexation efficiency of a metal ion M_{aq} by a given ligand is usually assessed by the pM (= $-\log [M_{aq}]$) value calculated at physiological pH for total concentrations of $[M]_{tot} = 10^{-6}$ M and $[L]_{tot} = 10^{-5}$ M.[47] In the case of **Tsox**, this translates into pLn values of 15.9 (La), 15.6 (Eu), and 15.1 (Lu), compared to pEu = 19.6 for $[Eu(dtpa)]^{2-}$ (dtpa = diethylenetriaminopentaacetic acid) or 8.1 for [Eu(8-hydroxyquinoline)$_3$], as computed from known stability constants.[48] The chelate effect of the podand with respect to the 8-hydroxyquinoline building block is impressive and the complexes based on **Tsox** appear to be sufficiently stable in water for potential in vivo applications.

Similar to the work performed on **Tsox**, the speciation in equimolar solutions of **TsoxMe** and Eu^{III} has been established. The cumulative stability constants are reported in Table 2, and the calculated pEu value is 14.9. Therefore, methylation of the amide groups only slightly weakens the coordination ability of **TsoxMe** compared with that of **Tsox**, and the loss of stability is acceptable, given the much better photophysical properties of the corresponding chelates (see below).

(45) Bravard, F.; Rosset, C.; Delangle, P. *Dalton Trans.* **2004**, 2012−2018.
(46) Imbert, D.; Fatin-Rouge, N.; Bünzli, J.-C. G. *Eur. J. Inorg. Chem.* **2003**, 1332−1339.
(47) Raymond, K. N.; Müller, G.; Matzanke, F. *Top. Curr. Chem.* **1984**, *123*, 49−102.
(48) Martell, A. E.; Smith, R. M. *Critical Stability Constants*; Plenum Press: New York, 1974.

Table 3. Ligand-Centered Absorption and Emission Properties of **Tsox** (pH 13) and of the $[Ln(H_2L)]^{3-}$ Podates (Ln = La, Gd, Eu, Lu) at pH 7.4

Ln	E ($^1\pi\pi^*$) (cm^{-1}) [a]	E ($^3\pi\pi^*$) (cm^{-1}) [b]	ΔE (cm^{-1}) [c]	τ (ms)[d]
$[HL]^{8-}$	*21 410*	19 570, *19 040*, 18 000	6600	225(14)
$[LaH_2L]3^-$	*21 290*	18 830, *18 270*, 17 140	7600	34(1)
$[GdH_2L]^{3-}$	*22 540*	19 260, *18 700*, 16 690	7900	0.8(1)
$[EuH_2L]^{3-}$	*21 820*			0.96(9)
$[LuH_2L]^{3-}$	*21 310*	18 780, *18 150*, 16 972	7800	22(1)

[a] From fluorescence spectra at 295 K, maximum of the band envelope. [b] From phosphorescence spectra at 77 K; maxima of the band envelopes are italicized. [c] Energy difference between the $^1\pi\pi^*$ and $^3\pi\pi^*$ ligand levels. [d] Lifetimes at 77 K of the ligand $^3\pi\pi^*$ states and, for the Eu complex, of the $^5D_0$ excited level (analysis on the $^5D_0 \rightarrow {}^7F_2$ transition).

Photophysical Properties of Tsox and its Complexes. In water, the absorption spectrum of **Tsox** features three main bands located around 48 800, 37 300, and 29 000 cm^{-1} (Figure 3). They are assigned to $\pi \rightarrow \pi^*$ and n $\rightarrow \pi^*$ transitions and are shifted, on going from the acidic to the basic forms of **Tsox**. The low-energy absorption band is slightly blue shifted (670 cm^{-1}), while the high-energy one is more sensitive to the deprotonation process, being successively red shifted ($\sim$1830 cm^{-1}) until pH $\sim$ 7.5 and then blue shifted by 530 cm^{-1} at pH 12.5, with respect to its energy at pH 1.7. In the Ln^{III} complexes, the more energetic band is slightly blue-shifted ($\sim$320$-$400 cm^{-1}). The photophysical properties of the ligand and of its 1:1 complexes with La, Gd, Eu, and Lu, both at room temperature in aqueous solutions and at 77 K in a frozen glycerol/water (10/90 v/v) mixture, are summarized in Table 3. At 295 K, UV excitation in the $\pi \rightarrow \pi^*$ and n $\rightarrow \pi^*$ absorption bands of the ligand results in a ligand-centered emission displaying one broad band assigned to the $^1\pi\pi^*$ state (21 410 cm^{-1}). At 77 K, the singlet-state emission disappears upon enforcement of a delay time. A second band appears, centered at 18 500 cm^{-1} and extending from 20 500 to 15 000 cm^{-1} (Figure 5), which corresponds to the $^3\pi\pi^*$ state emission, with a monoexponential decay of 225 ms. Because of the heavy atom effect, this lifetime decreases drastically in the corresponding Ln^{III} complexes. The ligand-centered luminescence of the lanthanide chelates $[Ln(H_2L)]^{3-}$ (Ln = La, Gd, Lu) displays essentially the same features except for slight shifts of the maxima. Complexes with the phosphorescent Eu^{III} and Tb^{III} ions behave differently. Because of the low energy of the ligand triplet state, with respect to the energy of the Tb($^5D_4$) level (20 450 cm^{-1}), no metal-centered luminescence occurs for the latter complex and the emission spectra are similar to the ones recorded for the nonluminescent Ln^{III} ions. In the case of the Eu^{III} complex with **Tsox**, $^3\pi\pi^*$ emission is not detected, and the characteristic narrow emission lines of the metal ions are observed, together with a residual emission from the $^1\pi\pi^*$ state, reflecting an efficient $^3\pi\pi^*-Eu^{III}$ transfer. However, the absolute quantum yield of $[Eu(H_2L)]^{3-}$ determined in water, $Q^L_{Eu} = 0.02\%$ (Table 4), is indicative of a rather weak sensitization of the Eu^{III} luminescence. This can be attributed to two reasons. First, ΔE ($^1\pi\pi^*-{}^3\pi\pi^*$) in **Tsox** (6600 cm^{-1}, calculated from the 0$-$0 transitions) is well above the optimum value (5000 cm^{-1}) for an efficient intersystem crossing process (isc),[49] as determined by the observation of a residual fluorescence from the ligand. Second, empirical rules have been proposed for an optimal ligand-to-metal transfer process,[50] 2500 < $\Delta E(^3\pi\pi^*-{}^5D_0)$ < 3500 cm^{-1}; in our case, the energy gap is much smaller, $\Delta E(^3\pi\pi^*-{}^5D_0) \approx 1480$ cm^{-1}, making temperature-dependent nonradiative processes and energy back transfer quite likely. Evidence for this is given by the lifetime of the Eu($^5D_0$) level which decreases from 0.96 $\pm$ 0.09 ms at 77 K to 3.9 $\pm$ 0.1 μs at room temperature.

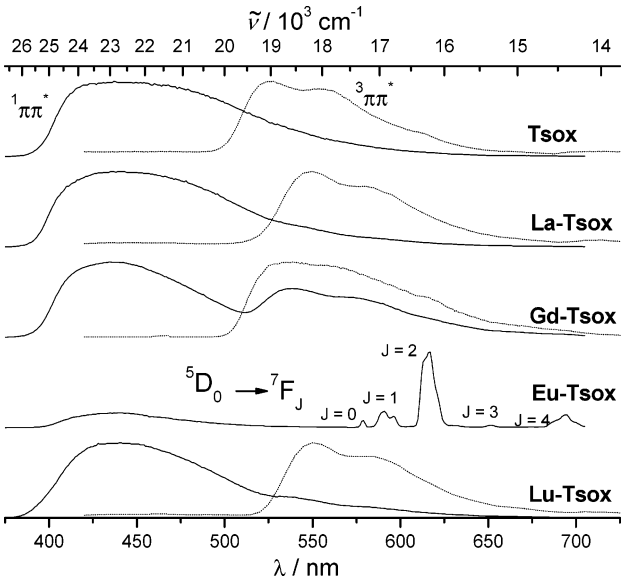

Figure 5. Luminescence spectra of **Tsox** and its 1:1 complexes 6×10^{-5} M in HBS buffer pH 7.4 containing 10% glycerol at 77 K without time delay (solid line) and with a 0.05 ms time delay (dotted line).

Table 4. Metal Ion-Centered Lifetimes (τ (μs)) for Nd ($^4F_{3/2}$), Yb ($^2F_{5/2}$), and Er ($^4I_{13/2}$) in the $[Ln(H_2L)]^{3-}$ Podates with **Tsox** (Ln = Nd, Er, Yb) at pH 7.4 (HBS buffer) in Water and D_2O Solution, Number of Water Molecules Bound in the Inner Coordination Sphere, and Absolute Quantum Yields (%)

			H_2O		D_2O		
T (K)	compd[a]	λ_{an} (nm)	τ (μs)	Q^L_{Ln} (%)	τ (μs)	Q^L_{Ln} (%)	q[b]
			Tsox				
295	$[NdH_2L]^{3-}$	1063	0.13(1)	0.02	0.58(2)	0.10	0.37
	$[YbH_2L]^{3-}$	976	2.21(1)	0.18	10.0(1)	0.81	0.15
	$[ErH_2L]^{3-}$	1540	0.23(1)	3.7×10^{-5}	1.39(2)	5.4×10^{-3}	
10	$[NdH_2L]^{3-}$	1063			0.59(1)		
	$[YbH_2L]^{3-}$	976			12.7(3)		
	$[ErH_2L]^{3-}$	1540			1.44(2)		
			TsoxMe				
295	$[NdH_2L]^{3-}$	1063	0.25(3)	0.04	0.61(1)	0.11	-0.09
	$[YbH_2L]^{3-}$	976	5.79(1)	0.37	14.6(1)	0.90	-0.1
	$[ErH_2L]^{3-}$	1540	0.67(1)	4.0×10^{-5}	2.31(2)	7.1×10^{-3}	
			Tsox + Triton X-100[c]				
295	$[YbH_2L]^{3-}$	976	2.82(1)	0.19			
			TsoxMe + Triton X-100[c]				
295	$[YbH_2L]^{3-}$	976	6.42(3)	0.37			

[a] $[LnH_2L]^{3-} = 6.0 \times 10^{-5}$ M (Ln = Er, Yb, Nd). [b] From eqs 13 and 14. [c] [Triton X-100] = 6.0×10^{-3} M.

(49) Steemers, F. J.; Verboom, W.; Reinhoudt, D. N.; Vandertol, E. B.; Verhoeven, J. W. *J. Am. Chem. Soc.* **1995**, *117*, 9408−9414.
(50) Latva, M.; Takalo, H.; Mukkala, V. M.; Matachescu, C.; Rodriguez-Ubis, J.-C.; Kankare, J. *J. Lumin.* **1997**, *75*, 149−169.

The overall sensitization process of Ln-centered luminescence is given by[38]

$$Q_{Ln}^{L} = \eta_{sens} Q_{Ln}^{Ln} = \eta_{isc} \eta_{et} Q_{Ln}^{Ln} = \eta_{isc} \eta_{et} \frac{\tau_{obs}}{\tau_{rad}} \qquad (11)$$

where Q_{Ln}^{L} is the quantum yield upon ligand excitation, η_{sens} is the efficiency of the overall ligand-to-metal energy transfer, η_{isc} is the efficiency of the intersystem crossing, η_{et} is the efficiency of the $^3\pi\pi^*-$Ln energy transfer, and Q_{Ln}^{Ln} is the intrinsic quantum yield (i.e., the quantum yield obtained upon direct Ln^{III} excitation). In the case of Eu^{III}, the latter may be estimated from[51]

$$Q_{Eu}^{Eu} = \tau_{obs} A_{MD,0} n^3 \cdot \frac{I_{tot}}{I_{MD}} \qquad (12)$$

where τ_{obs} is the observed lifetime of the Eu($^5D_0$) level, τ_{rad} is the radiative lifetime (i.e., the lifetime in the absence of any nonradiative process), $A_{MD,0} = 14.65\ s^{-1}$ is the spontaneous emission probability of the magnetic dipole $^5D_0 \rightarrow {}^7F_1$ transition, n is the refractive index, I_{tot} is the integrated emission of the $^5D_0 \rightarrow {}^7F_J$ ($J = 0-6$) transitions, and I_{MD} is the integrated emission of the $^5D_0 \rightarrow {}^7F_1$ transition. Analysis of the 295 K data (Table 4) leads to $Q_{Eu}^{Eu} \approx 0.22\%$ with a low value for η_{sens} (0.09). A rough estimate of the intersystem crossing efficiency, from the fluorescence spectra of the ligand at low temperature, gives $\eta_{isc} = 0.17$ allowing calculation of the $^3\pi\pi^*-$Ln transfer efficiency, $\eta_{et} \approx 0.5$. The relatively large value of τ_{obs} at 77 K is indicative of the probable absence of water molecules bound in the inner coordination sphere of the Eu^{III} ion, a fact corroborated by very similar Eu($^5D_0$) lifetimes obtained at room temperature for solutions in water and deuterated water. The presence of efficient temperature-dependent nonradiative deactivation processes different from luminescence quenching by high-energy vibrations prevents the evaluation of the number of water molecules directly bound to Eu^{III} by the usual method.[52]

Similar studies on the 1:1 complexes with deprotonated **Tox** (Ln = La, Gd, Eu, Lu; Figure S9, Supporting Information) in methanol (these complexes are not soluble in water) and with **TsoxMe** in water, display parallel trends. These experiments demonstrate that neither the sulfonation of the 5 position of the 8-hydroxyquinoline building blocks nor the methylation of the tren subunits influence the energy of the ligand emissive states. Since **Tsox** and **TsoxMe** possess low-energy triplet states, it appears that they will be well-suited for the sensitization of the lanthanide ions emitting in the NIR range.

Sensitization of Lanthanide-Centered NIR Emission by Tsox and TsoxMe. All chelates of **Tsox** [27] and **TsoxMe** (Figure 6) with Nd^{III}, Er^{III}, and Yb^{III} display sizable metal-centered NIR luminescence in aqueous solutions at pH 7.4. In addition, ligand emission contributes only faintly to the luminescence spectra, mainly through fluorescence from the singlet state with an intensity at least 10 times smaller than that of the free ligands, which indicates an efficient energy transfer process to the acceptor levels of the metal ions. Sensitization of the NIR luminescence by the ligands is ascertained by the excitation spectra which closely match the absorption spectra (Figure 6).

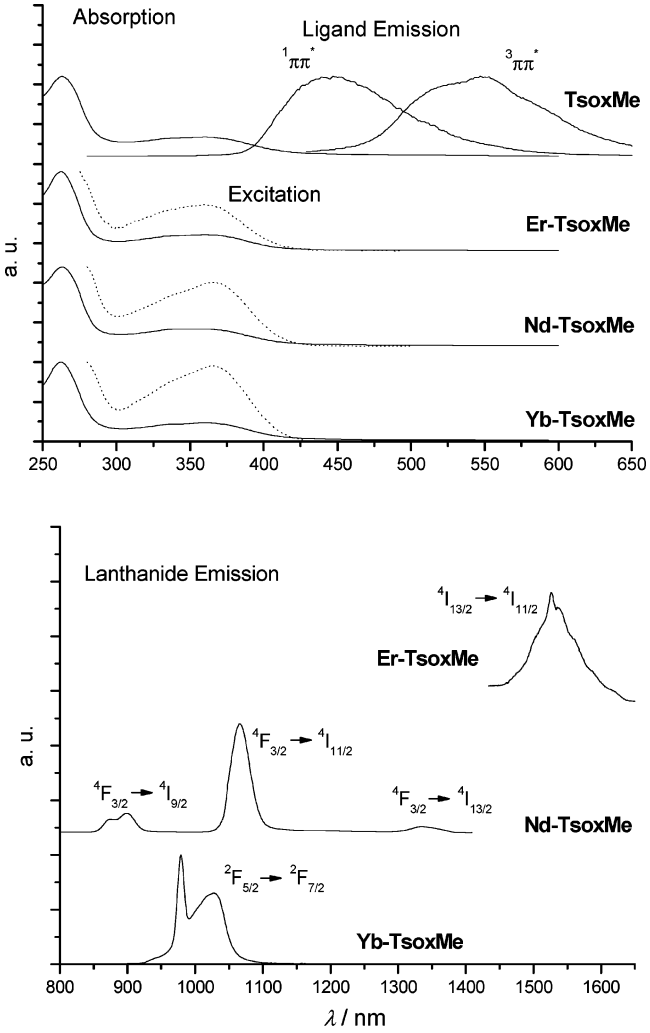

Figure 6. (top) Normalized absorption, emission ($\lambda_{ex} = 344$ nm), and excitation spectra (dotted line, $\lambda_{an} = 1540$ (Er), 1063 (Nd), and 976 nm (Yb)) and (bottom) emission spectra in the NIR region ($\lambda_{ex} = 344$ nm) of the 1:1 chelates of Er^{III}, Nd^{III}, and Yb^{III}. All solutions are in water at pH 7.4 and room temperature.

At room temperature and upon broad band excitation through both ligand levels at 267 (37 450 cm^{-1}) and 344 nm (29 070 cm^{-1}), the luminescence spectra are identical and display peaks corresponding to the expected f−f NIR transitions. The $[Yb(H_2L)]^{3-}$complex is characterized by a band in the 920−1100 nm range, assigned to the $^2F_{5/2} \rightarrow {}^2F_{7/2}$ transition, with a sharp main component at 976 nm and broader components at longer wavelengths due, in part, to vibronic transitions.[53] The $[Nd(H_2L)]^{3-}$ complex displays three bands in the 845−1408 nm range, the main band occurring between 1010 and 1140 nm ($^4F_{3/2} \rightarrow {}^4I_{9/2}$), with a maximum at 1064 nm; two other bands are visible between

(51) Werts, M. H. V.; Jukes, R. T. F.; Verhoeven, J. W. *Phys. Chem. Chem. Phys.* **2002**, *4*, 1542−1548.
(52) Supkowski, R. M.; Horrocks, W. deW. Jr. *Inorg. Chim. Acta* **2002**, *340*, 44−48.
(53) Platas, C.; Avecilla, F.; de Blas, A.; Rodriguez-Blas, T.; Geraldes, C. F. G. C.; Tóth, E.; Merbach, A. E.; Bünzli, J.-C. G. *J. Chem. Soc., Dalton Trans.* **2000**, 611−618.

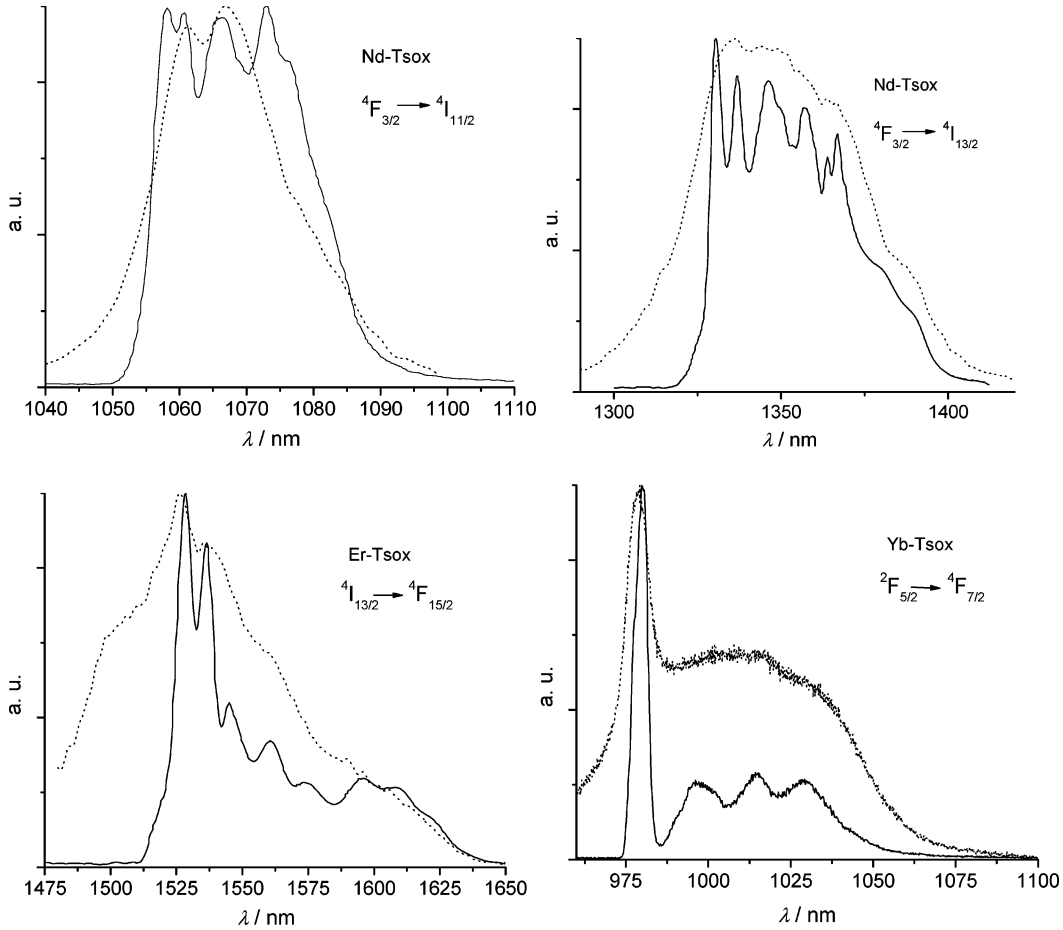

Figure 7. Emission spectra in the NIR region (λ_{ex} = 355 nm) of the 1:1 Ln^{III} chelates with **Tsox** (Ln = Nd, Er, Yb) at room temperature in deuterated water (dotted line) and at 10 K in a glycerol/deuterated water solution 10:90% (full line) at pH 7.4 in HBS buffer.

845−925 ($^4F_{3/2} \rightarrow {}^4I_{11/2}$) and 1290−1400 nm ($^4F_{3/2} \rightarrow {}^4I_{13/2}$). Finally, $[Er(H_2L)]^{3-}$ emits a band centered at 1540 nm, assigned to the $^4I_{13/2} \rightarrow {}^4I_{15/2}$ transition. When water is replaced by deuterated water, the luminescence spectra of the complexes described above remain essentially unchanged. With decreasing temperature, metal-centered emission bands become shaper and more structured as the vibronic contribution loses intensity, revealing the crystal-field splitting (Figure 7). For example, in the case of Yb^{III}, the irreducible representation of the angular momentum operator predicts four sublevels for Yb($^2F_{7/2}$) in low symmetry, and the corresponding transitions from the $^2F_{5/2}$ level are indeed observed at 979, 996, 1014, and 1029 nm, which corresponds to a total crystal-field splitting of 528 cm^{-1}; for comparison, a smaller total splitting of 372 cm^{-1} has been reported for a D_3-symmetrical bimetallic helicate,[54] consistent with the higher symmetry of the metal ion site.

The luminescence decays obtained upon excitation through the **Tsox** electronic levels are single-exponential functions of time, both in water and deuterated water, and the corresponding lifetimes of the Nd($^4F_{3/2}$), Yb($^2F_{5/2}$) and Er($^4I_{13/2}$) excited states are reported in Table 4. In deuterated water, the lifetimes are noticeably longer (0.58(2), 1.39(2), and 10.0(1) μs for Nd^{III}, Er^{III}, and Yb^{III}, respectively), reaching values comparable to those reported for polyaminocarboxylate complexes derived from dtpa (0.58, 1.46, and 10.4 μs, respectively).[23] To check temperature dependence, the lifetimes have also been measured at 10 K in a glycerol/D_2O mixture and were essentially found to be identical to the ones determined at room temperature in D_2O (except for a 25% increase in the case of Yb). This means that temperature-dependent deactivation processes are minimized in these podates, and therefore, **Tsox** is an adequate ligand forming an induced protective coordination environment around the metal ion. In the case of Nd^{III} and Yb^{III}, lifetime data allows one to determine the number of bound water molecules, q, by use of eq 13 for Nd^{III}, proposed by Faulkner et al.[21,55] and calibrated with polyaminocarboxylate complexes with $q = 0-2$, and of eq 14 for Yb^{III}, proposed by Beeby et al.[56] on the basis of complexes in solution with $q \leq 1$

$$q = A(\Delta k_{obs}) - C \text{ for } Nd^{III} \quad (13)$$

$$q = A(\Delta k_{obs} - B) \text{ for } Yb^{III} \quad (14)$$

where A = 130 ns (Nd^{III}) and 1 μs (Yb^{III}), C = 0.4, and B

(54) Gonçalves e Silva, F. R.; Malta, O. L.; Reinhard, C.; Güdel, H. U.; Piguet, C.; Moser, J. E.; Bünzli, J.-C. G. *J. Phys. Chem. A* **2002**, *106*, 1670−1677.

(55) Faulkner, S.; Beeby, A.; Carrié, M.-C.; Dadabhoy, A.; Kenwright, A. M.; Sammes, P. G. *Inorg. Chem.* Commun. **2001**, *4*, 187−190.

$= 0.2\ \mu s^{-1}$; $k_{obs} = 1/\tau_{obs}$ (expressed in μs^{-1} and ns^{-1} for Yb^{III} and Nd^{III}, respectively) and $\Delta k_{obs} = k_{obs}(H_2O) - k_{obs}(D_2O)$. In this way, we obtain $q = 0.37$ and 0.15 for Nd^{III} and Yb^{III}, respectively. These values are close to 0 and their residual value can come (i) from contributions of either second-sphere water molecules or proximate N−H or C−H oscillators[56] or (ii) from an equilibrium involving a monohydrated species. The situation clarifies itself when considering the lifetimes measured for the **TsoxMe** chelates (Table 4), which are 2−3 times larger for aqueous solutions than the lifetimes of the **Tsox** chelates, while the increase for deuterated solutions is considerably less pronounced. The calculated values of q are now around −0.1, essentially zero. An obvious conclusion is that the residual q values observed with **Tsox** do come from a nonradiative deactivation induced by the proximate N−H groups. Consequently, we can safely conclude that the Ln^{III} inner coordination sphere is saturated by the four pendant arms of the podand which acts as an octadentate host and that water molecules are excluded from the inner coordination sphere.

To quantify the ability of the chromophoric subunits of **Tsox** to sensitize the NIR-emitting lanthanides, the absolute quantum yields of the Ln^{III} podates (Ln = Nd, Er, Yb) in H_2O and D_2O solutions have been determined upon ligand excitation and under experimental conditions (6.0×10^{-5} M solutions buffered at pH 7.4) for which we have established above that the major species is the $[Ln(H_2L)]^{3-}$ complex. The quantum yields are 0.02 and 0.18% for Nd^{III} and Yb^{III}, respectively, and they increase by more than a factor four in deuterated water (Nd, 0.1%; Yb, 0.81 %) consistent with the trend observed in the lifetimes. The NIR luminescence of the Er^{III} chelate is sufficiently intense at room temperature for allowing the calculation of a quantum yield of 3.7×10^{-5}% which strongly increases in deuterated water (5.4×10^{-3}%). All of these quantum yields are sizable with respect to published literature data (vide supra), particularly for Yb^{III} and for aqueous solutions in which the presence of proximate OH vibrations often induces a large quenching effect for the ions having a small energy gap, which does not appear to be the case here. To calculate the efficiency of the sensitizing process with eq 11, we need to know the radiative lifetime values, which are not easy to determine experimentally. Literature data for τ_{rad} for the ions investigated, Nd^{III}, Er^{III}, and Yb^{III}, vary widely and depend heavily on the solvent or the physical state of the sample:[23,57−59] for instance, data ranging from 0.66 (aqua ion) to 14 ms (in dmso) are reported for Er^{III}. Taking into account the aqua-ion values (0.42 ms for Nd and 0.66 ms for Er) proposed by W. T. Carnall[57] and a value of 2 ms commonly assumed for Yb,[59] the data for aqueous solutions point to $\eta_{sens} \approx 0.7$ for Nd and < 0.01 for Er, while a value > 1 is obtained for Yb, meaning that the actual radiative lifetime is larger than 2 ms in our system.

Similar experiments have been carried out on the ligand **TsoxMe**, and the results are also reported in Table 4. We note that at room temperature, the absolute quantum yields of the $[Ln(H_2L)]^{3-}$ podates in aqueous solutions increase by a factor two when the methyl groups replace the hydrogen atoms, consistent with the concomitant increase in the lifetimes: a quantum yield as high as 0.37% is obtained for the Yb^{III} chelate. The quantum yields of solutions in deuterated water do not sustain the same increase in quantum yield on going from **Tsox** to **TsoxMe** (+10% vs 2-fold), in line with the above discussion on nonradiative deactivation processes pointing to the N−H groups being the major contributors to nonradiative deactivation induced by proximate groups, either within the chelate molecule or through second-sphere solvent interaction. That the latter is minimized is confirmed by the introduction of a surfactant in the solutions. Indeed, several studies describe an increase in the luminescence of metal complexes by inserting them in micelles.[60,61] Therefore, one hundred equivalents of Triton X-100 have been added to solutions of the Yb^{III} complexes with **Tsox** and **TsoxMe**. No significant increase in the overall quantum yield has been obtained. An explanation is that the podands used not only saturate the first coordination sphere of the metal ions but, in addition, build an hydrophobic shell around the inner coordination sphere minimizing second-sphere interactions with water.

Extending the Excitation Wavelength. A close scrutiny of the absorption spectra of the chelates reveals that the long wavelength band is in fact tailing off up to about 700 nm. Although absorbance is quite low, we have attempted to excite the Yb^{III} chelates with visible light, using argon laser lines at 465.8, 514, and 580 nm. NIR luminescence is indeed detected at 976 nm. To investigate whether this excitation mode follows the regular one-photon mechanism, as opposed to two-photon excitation,[62] we have measured the luminescence intensity versus the power of the laser (see Figures S10 and S11 for **Tsox** and S12 for **TsoxMe)**. Regardless of the excitation wavelength (355, 514, and 580 nm), the resulting plots are linear with a slope close to one (0.91, 1.02, 0.99 for **Tsox** and 0.94, 1.03, and 1.08 for **TsoxMe**), pointing to one-photon excitation.

Conclusion

The solution studies described in this paper show that podands **Tsox** and **TsoxMe** lead to soluble and thermodynamically stable Ln^{III} complexes in water, featuring resistance toward hydrolysis, with pLn values in the range of 14−16. A single major species is present at physiological pH, the 1:1 podate $[Ln(H_2L)]^{3-}$ which presents interesting photo-

(56) Beeby, A.; Clarkson, I. M.; Dickins, R. S.; Faulkner, S.; Parker, D.; Royle, L.; de Sousa, A. S.; Williams, J. A. G.; Woods, M. *J. Chem. Soc., Perkin Trans. 2* **1999**, 493−503.
(57) Carnall, W. T. In *Handbook on the Physics and Chemistry of Rare Earths*; Gschneidner, K. A., Jr., Eyring, L., Eds.; North-Holland Publ. Co.: Amsterdam, 1979; Vol. 3, Chapter 24, 172.
(58) Weber, M. J. *Phys. Rev.* **1968**, *171*, 283−291.
(59) Klink, S. I.; Grave, L.; Reinhoudt, D. N.; Van Veggel, F. C. J. M.; Werts, M. H. V.; Geurts, F. A. J.; Hofstraat, J. W. *J. Phys. Chem. A* **2000**, *104*, 5457−5468.
(60) Hemmilä, I.; Ståhlberg, T.; Mottram, P. *Bioanalytical Applications of Labeling Technologies*; Wallac Oy: Turku, Finland, 1995.
(61) Walworth, J.; Brewer, K. J.; Richter, M. M. *Anal. Chim. Acta* **2004**, *503*, 241−245.
(62) Fu, L. M.; Wen, X. F.; Ai, X. C.; Sun, Y.; Wu, Y. S.; Zhang, J. P.; Wang, Y. *Angew. Chem., Int. Ed.* **2005**, *44*, 747−750.

physical properties in the NIR range, particularly for Ln = Nd and Yb. The lifetimes of the excited states of these metal ions, as well as quantum yields determined in H_2O and D_2O, point to the absence of water molecules in the first coordination sphere and to a minimization of second-sphere interactions. Thus the molecular design adopted here meets all the requirements for bioanalytical luminescent probes. Indeed, 8-hydroxyquinolinate is known to efficiently sensitize the luminescence of NIR-emitting lanthanide ions, but on the other hand, the stoichiometry of simple lanthanide quinolinates is difficult to control and a variety of mono, bi-, and trimetallic structures are obtained depending on the experimental conditions used.[63,64] In the study presented here, the 8-hydroxyquinoline moieties have been inserted into a carefully tailored podand so that a single and highly protective environment is induced upon complexation, as demonstrated by the absence of water in the inner coordination sphere, even in aqueous solution. This represents a decisive advantage on the above-mentioned compounds. As a result, the quantum yield displayed by the Yb−**TsoxMe** chelate is quite sizable, being for instance 4- and 15-fold larger than the ones reported for complexes with fluorexon[16] and tropolonate,[18] respectively. The overall efficiency of a luminescent probe is given by the factor ϵQ_{Ln}^{L}, which takes into account the amount of light that can be harvested by the ligand. With molar absorption coefficients at 267 and 344 nm of 92 200 and 19 400 M^{-1} cm^{-1} for **Tsox** and 74 800 and 18 950 M^{-1} cm^{-1} for **TsoxMe**, ϵQ_{Ln}^{L} = 166 and 35 M^{-1} cm^{-1} for the Yb−**Tsox** chelate and 277 and 70 M^{-1} cm^{-1} for the Yb−**TsoxMe** complex. The latter data compare favorably with the bimetallic complex with 1,10-phenanthroline substituted in the 2 and 9 positions by benzoazacyclic moieties (113 and 87 M^{-1} cm^{-1} at 245 and 280 nm for a quantum yield of 0.53%).[24] In addition, the possibility of excitation in the visible range is a definitive asset for probes intended for bioanalyses. Altogether, this molecular engineering opens astounding perspectives for the development of luminescent bioprobes since the synthesis of **TsoxMe** can be undertaken on large scale effortlessly and derivatization of this chelating agent is also easily at hand, in particular with respect to the grafting of functional groups for the coupling with large biological molecules. Experiments toward this goal are in progress in our laboratory.

Acknowledgment. This research is supported through grants from the Swiss National Science Foundation. We thank Mr. Frédéric Gumy for his help in luminescence measurements.

Supporting Information Available: Synthesis of the ligands, potentiometric titration curve and data for the UV−vis titration of **Tsox** (Figures S1−S5) and of **Tsox** in the presence of 1 equiv of Eu^{III} (Figures S6−S8), luminescence spectra of **Tox** and its 1:1 complexes (Figure S9), luminescence intensity of the Yb−**Tsox** (Figures S10 and S11) and Yb−**TsoxMe** (Figure S12) complexes versus laser power. This material is available free of charge via the Internet at http://pubs.acs.org.

IC0515249

(63) Van Deun, R.; Fias, P.; Nockemann, P.; Schepers, A.; Parac-Vogt, T. N.; Van Hecke, K.; Van Meervelt, L.; Binnemans, K. *Inorg. Chem.* **2004**, *43*, 8461−8469.

(64) Artizzu, F.; Deplano, P.; Marchio, L.; Mercuri, M. L.; Pilia, L.; Serpe, A.; Quochi, F.; Orru, R.; Cordella, F.; Meinardi, F.; Tubino, R.; Mura, A.; Bongiovanni, G. *Inorg. Chem.* **2005**, *44*, 840−842.